The added mass for two-dimensional floating structures

McIver, M. & McIver, P.

Department of Mathematical Sciences, Loughborough University, Loughborough, Leicestershire, LE11 3TU, UK.

Abstract

The diagonal terms in the added mass matrix for a two-dimensional surface-piercing structure, which satisfies a geometric condition known as the John condition, are proven to be non-negative. It is also shown that the heave coefficient, associated with a symmetric system of two such structures, is non-negative when the length of the free surface connecting the structures lies between an odd, and the next higher even, number of half-wavelengths. The sway and roll coefficients, associated with antisymmetric motion of the system, are non-negative in the complementary intervals. For a specific geometry these intervals are equivalent to frequency ranges. Negative added mass is associated with rapid variations with frequency, due to complex resonances that correspond to simple poles of the associated radiation potential in the complex frequency domain. Approximate techniques are used to show that, for systems of two structures, complex resonances are located at frequencies consistent with the intervals in which negative added mass is able to occur.

Keywords: Linear water waves, Added mass, John condition, Complex resonance

1. Introduction

This paper is concerned with the linearised theory of the interaction between water waves and a floating structure that is constrained to move with a single degree of freedom. In the frequency-domain radiation problem [1, Chapter 1], when the structure is forced to perform time-harmonic oscillations, the complex-valued hydrodynamic force on the structure is written as the sum of a part proportional to minus the velocity of the structure, and a part proportional to minus its acceleration. The respective coefficients of proportionality are usually termed the damping matrix and the added mass matrix and the diagonal terms of these matrices represent the

Email address: m.mciver@lboro.ac.uk (McIver, M. & McIver, P.)

components of the force in the same direction as the mode of oscillation. In what follows we shall concentrate only on these diagonal terms and refer to them simply as the damping and added mass.

From energy flux considerations the damping is necessarily non-negative, but there is no corresponding physical restriction on the added mass. While for many structures the added mass has been found to be positive for all frequencies, there are particular structures for which the added mass becomes negative over one or more ranges of frequencies. Some of the earliest reported calculations of negative added mass were for the two-dimensional geometry of a cylinder that is close to the free surface [2]. Subsequently, negative added mass has been found for other shallowly-submerged structures including a rectangular cylinder [3], a vertical circular cylinder [4] and a horizontal disc [5]. Another class of structure for which negative added mass may occur is one where one or more elements of the structure enclose a portion of the free surface. Geometries in this class include a pair of surface-piercing cylinders in two dimensions [6, 7, 8, 9], and toroidal structures in three dimensions [10, 11, 12]. Most of the calculations mentioned above are for the heave motion of the structure, but some examples of negative added mass are reported for other modes of motion such as surge and pitch [10].

In general, negative added mass is associated with rapid variations with frequency of the hydrodynamic force. In turn these variations can be attributed to the resonances associated with weakly-damped standing waves that occur near certain frequencies or, in some cases, a low-frequency pumping mode (known as the piston mode or Helmholtz mode) that is associated with a localised near-vertical motion of the fluid [7, 8]. That these motions are possible is perhaps more readily apparent when the structure encloses a portion of the free surface such as in [10, 8], but similar interpretations can be made for submerged structures [3, 4]. Another situation where near-resonant standing waves occur is when an oscillating structure is placed between parallel rigid walls. Thus negative added mass has been found for a swaying vertical cylinder in a channel [13], even though the added mass is positive at all frequencies when the cylinder is placed in open water.

The near-resonant motions just described are the physical manifestations of simple poles in the frequency-domain radiation potential, when it is regarded as a function of complex frequency. The locations of these poles are known as complex resonances or scattering frequencies, and their real and imaginary parts determine the frequency and damping rate of the resonant mode respectively. The residue of the complex potential at a pole, describes the corresponding fluid motion when the mode is excited in the time domain [14]. Each complex resonance of a radiation potential corresponds directly to a complex resonance of the force coefficient, the real part of

which is the added mass coefficient and the imaginary part the damping. A simple pole of this force coefficient that is close to the real axis gives a mathematical description of the rapid changes that are observed in the added mass and damping coefficients near resonance [13, 5]. The contributions of the present work are to provide conditions under which negative added mass is impossible and, in situations where it is possible, to obtain approximations to the complex resonances and their associated residues.

When a simple harmonic wave is incident on a fixed structure of non-zero volume, that satisfies the geometric condition defined in §2, McIver [15] demonstrated that the time-averaged potential energy in the fluid is less than or equal to the time-averaged kinetic energy, using the method introduced by John [16]. Energy conservation in the fluid then leads to the result, that such a structure cannot be transparent to an incident wave but always produces a scattered wave field. A similar argument is used in this work, to show that the time-averaged potential energy in the fluid is less than or equal to the time-averaged kinetic energy for such a structure, when it oscillates in a single mode of motion. Falnes & McIver [17] showed that the added mass is proportional to the difference in the potential and kinetic energies and so it follows that the added mass cannot be negative for such a structure at any frequency. The method of Linton & Kuznetsov [18] is then used to investigate a pair of structures, that individually satisfy the geometric condition defined in §2, and form a symmetric system that moves in tandem. Regions in the frequency domain in which the added mass cannot be negative are shown to be complementary for symmetric and antisymmetric modes of motion. Calculations are made of the added mass for a pair of circular cylinders that are half immersed in water of infinite depth. The numerical results are consistent with the theoretical results and show that negative added mass occurs outside these regions, although its existence has not been proven.

The work on complex resonances in section 4 concentrates on a pair of identical symmetric structures. A wide-spacing assumption is used together with high-frequency asymptotics to obtain approximations to the locations of the resonances and the corresponding residues. As well as more general expressions, specific results are given for a pair of half-immersed cylinders and comparisons are made with numerical calculations.

2. Formulation

A two-dimensional, surface-piercing, piecewise-smooth structure makes small amplitude oscillations at angular frequency ω in water of constant depth h. Rectangular Cartesian coordinates are defined so that the z-axis points vertically upwards and

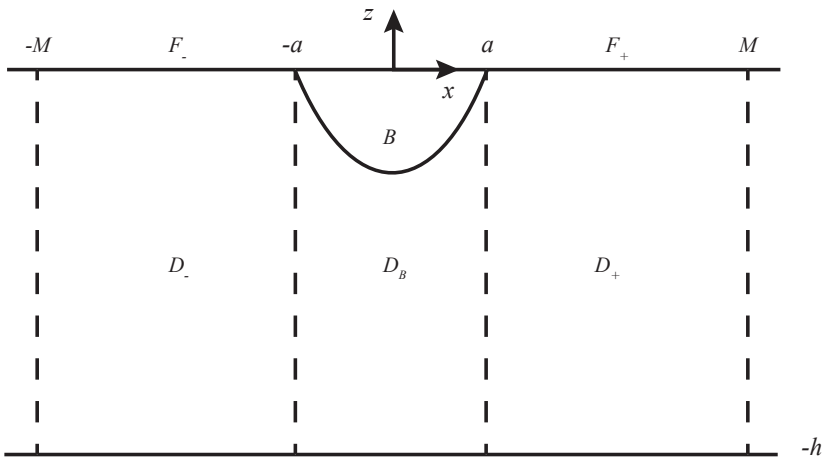

Figure 1: A single structure which satisfies the John condition

the mean free surface coincides with the line $z = 0$, as illustrated in Figure 1. In its equilibrium position, the structure is assumed to intersect this line only at the two points $(\pm a, 0)$, and to be such that a vertical line drawn down through the fluid from each point on the mean free surface does not intersect the structure. The portion of the free surface $-M < x < -a$ to the left of the structure is denoted by F_- and D_- is the fluid region below F_-. Similarly the portion of the free surface $a < x < M$ to the right of the structure is denoted by F_+ and D_+ is the fluid region below F_+. In the technical calculations that are made in §3, the limit as $M \to \infty$ will be taken, but a careful combination of certain integrals will need to be made before this limiting procedure is possible. So initially it is necessary to consider finite portions of the free surface on either side of the structure. The wetted boundary of the structure is denoted by B and the fluid region below the structure by D_B. The fluid is assumed to be inviscid and incompressible and the motion irrotational and sufficiently small for the linearised water wave theory to be valid. John [16] showed that the unforced frequency domain potential for such a body must be zero and so the structure will be said to satisfy the 'John condition'.

In two dimensions the frequency domain potential may be written as a linear combination of the potential due to the scattering of any incoming waves by a fixed structure and the potentials due to the radiation of waves by a structure making small horizontal and vertical oscillations in sway and heave respectively and roll

oscillations about an axis through the centre of rotation. Quantities associated with sway, heave and roll are designated by the suffices $p = 1, 3, 5$ respectively. If the component of the translation or rotational velocity in the pth mode of motion is given by $Re[v_p e^{-i\omega t}]$ then the corresponding velocity potential is $Re[v_p \phi_p(x, z) e^{-i\omega t}]$, where ϕ_p has continuous second partial derivatives in the fluid and is continuous onto the boundary. The potential ϕ_p satisfies

$$\nabla^2 \phi_p = 0, \quad \text{in the fluid} \tag{1}$$

and

$$\frac{\partial \phi_p}{\partial n} = n_p \quad \text{on the structure,} \tag{2}$$

where n_1 and n_3 are the components of the inward normal to the structure in the positive x and z directions respectively and $n_5 = (x - x_0)n_3 - (z - z_0)n_1$, where (x_0, z_0) denotes the centre of rotation. The linearised free surface boundary condition for ϕ_p is

$$K\phi_p - \frac{\partial \phi_p}{\partial z} = 0 \quad \text{on } z = 0, \quad x < -a, \ x > a, \quad K = \omega^2/g \tag{3}$$

and as there is no flow through the seabed,

$$\frac{\partial \phi_p}{\partial z} = 0 \quad \text{on } z = -h. \tag{4}$$

There are only outward propagating waves as $x \to \pm\infty$ and so

$$\phi_p \sim A_p^{\pm} e^{\pm ikx} \frac{\cosh k(z + h)}{\cosh kh} \quad \text{as} \quad x \to \pm\infty, \tag{5}$$

where the wave number k is related to the frequency parameter K through the dispersion relation

$$K = k \tanh kh. \tag{6}$$

The qth component of the hydrodynamic force on the structure due to the motion in mode p is obtained by integration of the oscillatory pressure multiplied by n_q over the mean wetted surface of the structure. The non-dimensional force coefficient is given by

$$q_{pq} = \mu_{pq} + i\nu_{pq} = \frac{1}{A_0} \int_B \phi_p \, n_q \, dS, \tag{7}$$

where A_0 is the cross-sectional area of the structure and the real quantities μ_{pq} and ν_{pq} are the non-dimensional added mass and damping matrices respectively.

It is well-known that the diagonal terms in the damping matrix are non-negative for all frequencies, as they represents the energy in the radiated waves. In the next

section, the method developed by John [16] to establish uniqueness of the velocity potential associated with this class of single two-dimensional structures, is used to show that the diagonal terms in the added mass matrix for these structures are non-negative at all frequencies. Negative added mass has been found numerically for symmetric pairs of surface-piercing structures that individually satisfy the John condition. However it will also be shown, that there are complementary bands of frequencies, in which the added mass associated with symmetric and antisymmetric motion for such a system of structures, is non-negative.

3. The sign of the added mass coefficient

3.1. A single structure

An application of the divergence theorem to $\phi_p \nabla \overline{\phi}_p + \overline{\phi}_p \nabla \phi_p$ in the fluid yields the relationship between the non-dimensional diagonal coefficient in the added mass matrix μ_{pp} and the difference between the time-averaged kinetic and potential energies derived by Falnes & McIver [17], namely

$$\mu_{pp} = \frac{1}{A_0} \lim_{M\to\infty} \left[\int_{D_- \cup D_+ \cup D_B} |\nabla \phi_p|^2 \, \mathrm{d}V - K \int_{F_- \cup F_+} |\phi_p|^2 \, \mathrm{d}x \right]. \tag{8}$$

To ensure convergence the integrals over the fluid domain and the mean free surface are taken together and the limit as $M \to \infty$ is taken. The aim here is to use the method described in [16] to show that the right-hand side of (8), hence μ_{pp}, is non-negative if the structure satisfies the John condition.

Green's theorem is applied to ϕ_p and $\mathrm{e}^{ik(x-s)} \cosh k(z+h)/\cosh kh$ in the region $x \geq s > a$. Both functions represent outward going waves as $x \to \infty$ and so the only contribution comes from the line $x = s$ and yields

$$\int_{-h}^{0} \left[\frac{\partial \phi_p}{\partial x} - \mathrm{i}k\phi_p \right]_{x=s} \frac{\cosh k(z+h)}{\cosh kh} \, \mathrm{d}z = 0. \tag{9}$$

The second term in (9) is integrated by parts and the equation rearranged to give

$$\begin{aligned}
\phi_p(s,0) &= \int_{-h}^{0} \left[\frac{\partial \phi_p}{\partial z} \frac{\sinh k(z+h)}{\sinh kh} - \mathrm{i} \frac{\partial \phi_p}{\partial x} \frac{\cosh k(z+h)}{\sinh kh} \right]_{x=s} \mathrm{d}z \\
&= \frac{1}{\sinh kh} \int_{-h}^{0} \left[\frac{\partial \phi_p}{\partial z} \cos\alpha - \mathrm{i} \frac{\partial \phi_p}{\partial x} \sin\alpha \right]_{x=s} \left(\sinh^2 k(z+h) + \cosh^2 k(z+h) \right)^{1/2} \mathrm{d}z \\
&= \frac{1}{2\sinh kh} \int_{-h}^{0} \left[\left(\frac{\partial \phi_p}{\partial z} - \frac{\partial \phi_p}{\partial x} \right) \mathrm{e}^{\mathrm{i}\alpha} + \left(\frac{\partial \phi_p}{\partial z} + \frac{\partial \phi_p}{\partial x} \right) \mathrm{e}^{-\mathrm{i}\alpha} \right]_{x=s} \left[\cosh 2k(z+h) \right]^{1/2} \mathrm{d}z,
\end{aligned} \tag{10}$$

where α is real and defined by the pair of equations

$$\begin{aligned}\cos\alpha &= \frac{\sinh k(z+h)}{(\sinh^2 k(z+h)+\cosh^2 k(z+h))^{1/2}},\\ \sin\alpha &= \frac{\cosh k(z+h)}{(\sinh^2 k(z+h)+\cosh^2 k(z+h))^{1/2}}.\end{aligned} \tag{11}$$

The Cauchy-Schwarz inequality is applied to the integral in (10) to give

$$\begin{aligned}|\phi_p(s,0)|^2 &\leq \frac{\int_{-h}^{0}\cosh 2k(z+h)\,\mathrm{d}z}{4\sinh^2 kh}\\ &\qquad\times\int_{-h}^{0}\left|\left(\frac{\partial\phi_p}{\partial z}-\frac{\partial\phi_p}{\partial x}\right)\mathrm{e}^{\mathrm{i}\alpha}+\left(\frac{\partial\phi_p}{\partial z}+\frac{\partial\phi_p}{\partial x}\right)\mathrm{e}^{-\mathrm{i}\alpha}\right|^2_{x=s}\mathrm{d}z\\ &\leq \frac{1}{2K}\int_{-h}^{0}\left[\left|\frac{\partial\phi_p}{\partial z}-\frac{\partial\phi_p}{\partial x}\right|^2+\left|\frac{\partial\phi_p}{\partial z}+\frac{\partial\phi_p}{\partial x}\right|^2\right]_{x=s}\mathrm{d}z\\ &= \frac{1}{K}\int_{-h}^{0}|\nabla\phi_p|^2_{x=s}\,\mathrm{d}z,\end{aligned} \tag{12}$$

after an application of the Cauchy inequality $|A+B|^2\leq 2\left(|A|^2+|B|^2\right)$ and the use of the dispersion relation (6). Integration of (12) over F_+ gives

$$K\int_{F_+}|\phi_p(x,0)|^2\,\mathrm{d}x\leq\int_{D_+}|\nabla\phi_p|^2\,\mathrm{d}V. \tag{13}$$

A similar analysis is applied in the region $x\leq s<-a$ and yields

$$K\int_{F_-}|\phi_p(x,0)|^2\,\mathrm{d}x\leq\int_{D_-}|\nabla\phi_p|^2\,\mathrm{d}V. \tag{14}$$

Substitution of (13) and (14) into (8) gives

$$\mu_{pp}\geq\frac{1}{A_0}\int_{D_B}|\nabla\phi_p|^2\,\mathrm{d}V\geq 0, \tag{15}$$

which means that the diagonal terms in the added mass matrix are non-negative for a single structure that satisfies the John condition in water of finite depth. If the region D_B has non-zero area then, as ϕ_p is not constant throughout such a region, the final inequality in (15) is strict and $\mu_{pp}>0$.

The results also holds in water of infinite depth, as was demonstrated in [19], by repeating the above analysis with $\cosh k(z+h)/\cosh kh$ replaced by e^{Kz} in (9) and noting that the infinite-depth wave number is given by $k = K$. However, numerical results show that it is possible for the added mass to be negative for a structure which doesn't satisfy the John condition, so it is not possible simply to dispense with this requirement. This is illustrated in Figure 2 where the sway added mass is given for a circular cylinder of radius a that is more than half-immersed in water of infinite depth and intersects the mean free surface at an angle of $\pi/4$ to the horizontal. It is clear that there is a range of frequencies near $Ka = 1$, for which the sway added mass is negative.

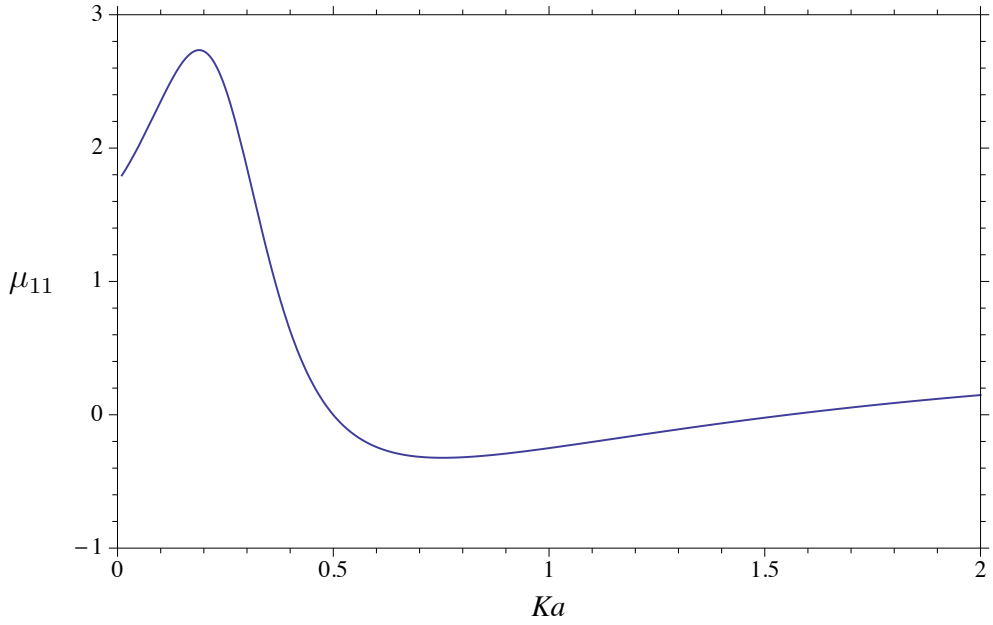

Figure 2: The sway added mass for a more than half-immersed circular cylinder

3.2. A symmetric system of two structures

A similar analysis may be performed for two structures that individually satisfy the John condition and form a symmetric configuration that oscillates in tandem, as illustrated in Figure 3. The method employed here is the same as that used by Linton & Kuznetsov [18] to determine ranges of frequencies for which symmetric and

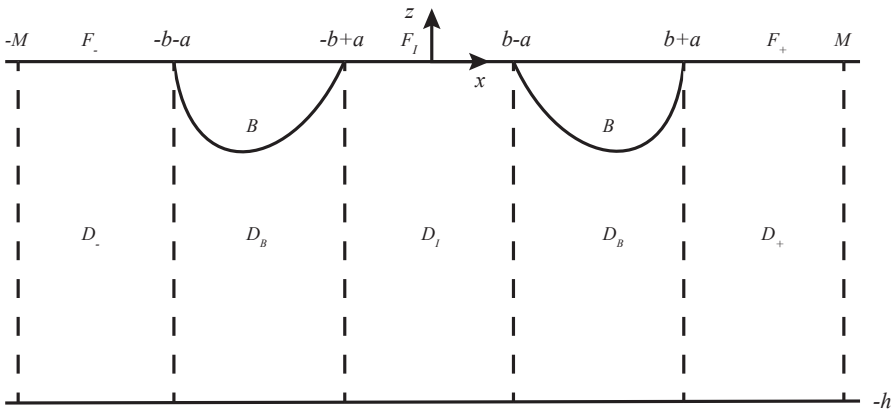

Figure 3: A symmetric configuration of two structures that individually satisfy the John condition

antisymmetric trapped modes are not supported by a symmetric configuration of two fixed structures.

As before the diagonal terms in the added mass matrix associated with the whole system moving as a single structure, are related to the difference in the time-averaged kinetic and potential energies in the fluid. So (8) becomes

$$\mu_{pp} = \frac{1}{A_0} \lim_{M\to\infty} \left[\int_{D_-\cup D_+\cup D_B\cup D_I} |\nabla\phi_p|^2 \,\mathrm{d}V - K \int_{F_-\cup F_+\cup F_I} |\phi_p|^2 \,\mathrm{d}x \right], \qquad (16)$$

where B and A_0 now represent the combined wetted boundaries and cross-sectional areas of the structures and D_B the combined fluid region below them both. The mean free surface between the structures is denoted by F_I and the fluid region below it by D_I. The same analysis as that used for the single structure shows that the inequalities (13) and (14) are satisfied and so (16) becomes

$$\begin{aligned} \mu_{pp} &\geq \frac{1}{A_0} \left[\int_{D_B\cup D_I} |\nabla\phi_p|^2 \,\mathrm{d}V - K \int_{F_I} |\phi_p|^2 \,\mathrm{d}x \right] \\ &\geq \frac{1}{A_0} \left[\int_{D_I} |\nabla\phi_p|^2 \,\mathrm{d}V - K \int_{F_I} |\phi_p|^2 \,\mathrm{d}x \right], \end{aligned} \qquad (17)$$

where the final inequality is strict if D_B has non-zero area. It remains to determine under what circumstances the right-hand side of (17) can be bounded below by zero, and this is done using the method described in [20, §4.2.2].

On the portion of the free surface between the structures the function w_p is defined by

$$w_p(x) = \int_{-h}^{0} \phi_p(x,z) \frac{\cosh k(z+h)}{\cosh kh} \, \mathrm{d}z. \tag{18}$$

The operator $\mathrm{d}^2/\mathrm{d}x^2$ is applied to (18) and the order of integration and differentiation changed. As ϕ_p satisfies the 2D Laplace equation the term $\partial^2\phi_p/\partial x^2$ may be replaced by $-\partial^2\phi_p/\partial z^2$ and the resulting integral integrated by parts twice. An application of the free surface boundary condition for ϕ_p in (3) shows that w_p satisfies

$$\frac{\mathrm{d}^2 w_p}{\mathrm{d}x^2} + k^2 w_p = 0. \tag{19}$$

The system of structures is symmetric about the z-axis and the centre of rotation is assumed to lie on this axis. So the heave potential ϕ_3 is symmetric in x and the sway and roll potentials, ϕ_1 and ϕ_5, are antisymmetric. This means that w_3 is a symmetric function and w_1 and w_5 are antisymmetric. It is convenient to consider the symmetric problem first.

From (18) and (19)

$$w_3(x) = \int_{-h}^{0} \phi_3(x,z) \frac{\cosh k(z+h)}{\cosh kh} \, \mathrm{d}z = B_3 \cos kx, \quad x \in F_I, \tag{20}$$

where B_3 is a complex constant. Integration of (20) by parts gives

$$\phi_3(x,0) = \frac{k^2}{K} B_3 \cos kx + \int_{-h}^{0} \frac{\partial \phi_3}{\partial z} \frac{\sinh k(z+h)}{\sinh kh} \, \mathrm{d}z, \tag{21}$$

after use of the dispersion relation (6). An application of the Cauchy inequality

$$|A+B|^2 = (1+\epsilon)|A|^2 + (1+1/\epsilon)|B|^2 - \left| \epsilon^{1/2} A - \frac{B}{\epsilon^{1/2}} \right|^2 \leq (1+\epsilon)|A|^2 + (1+1/\epsilon)|B|^2 \tag{22}$$

to (21), where ϵ is a positive parameter to be chosen, and multiplication by K gives

$$\begin{aligned} K\,|\phi_3(x,0)|^2 &\leq \frac{(1+\epsilon)k^4|B_3|^2\cos^2 kx}{K} + \frac{K(1+1/\epsilon)}{\sinh^2 kh} \left| \int_{-h}^{0} \frac{\partial \phi_3}{\partial z} \sinh k(z+h) \, \mathrm{d}z \right|^2 \\ &\leq \frac{(1+\epsilon)k^4|B_3|^2\cos^2 kx}{K} + \frac{K(1+1/\epsilon)\left[\sinh kh \cosh kh - kh\right]}{2k \sinh^2 kh} \int_{-h}^{0} \left| \frac{\partial \phi_3}{\partial z} \right|^2 \mathrm{d}z, \end{aligned} \tag{23}$$

where the Cauchy-Schwarz inequality has been used. Integration of (23) over F_I gives a bound for the potential energy associated with the portion of the free surface between the structures, namely

$$K\int_{F_I}|\phi_3(x,0)|^2\,\mathrm{d}x \le \frac{(1+\epsilon)k^3|B_3|^2\left[2k(b-a)+\sin 2k(b-a)\right]}{2K} + \frac{K(1+1/\epsilon)\left[\sinh kh\cosh kh-kh\right]}{2k\sinh^2 kh}\int_{D_I}\left|\frac{\partial\phi_3}{\partial z}\right|^2\mathrm{d}V. \quad (24)$$

The complex constant B_3 is unknown but differentiation of (20) with respect to x gives

$$-kB_3\sin kx = \int_{-h}^{0}\frac{\partial\phi_3}{\partial x}\frac{\cosh k(z+h)}{\cosh kh}\,\mathrm{d}z. \quad (25)$$

An application of the Cauchy-Schwarz inequality to (25), followed by integration over F_I produces the bound

$$\frac{k|B_3|^2\left[2k(b-a)-\sin 2k(b-a)\right]}{2} \le \frac{\left[\sinh kh\cosh kh+kh\right]}{2k\cosh^2 kh}\int_{D_I}\left|\frac{\partial\phi_3}{\partial x}\right|^2\mathrm{d}V. \quad (26)$$

Substitution of (26) into (24) gives

$$\begin{aligned} K\int_{F_I}|\phi_3(x,0)|^2\,\mathrm{d}x &\le \frac{(1+\epsilon)k^3|B_3|^2\sin 2k(b-a)}{K} \\ &+ \frac{(1+\epsilon)k\left[\sinh kh\cosh kh+kh\right]}{2K\cosh^2 kh}\int_{D_I}\left|\frac{\partial\phi_3}{\partial x}\right|^2\mathrm{d}V \\ &+ \frac{K(1+1/\epsilon)\left[\sinh kh\cosh kh-kh\right]}{2k\sinh^2 kh}\int_{D_I}\left|\frac{\partial\phi_3}{\partial z}\right|^2\mathrm{d}V. \quad (27) \end{aligned}$$

It is straightforward to show that the choice of the parameter ϵ as

$$\epsilon = \frac{\sinh kh\cosh kh-kh}{\sinh kh\cosh kh+kh} > 0 \quad (28)$$

means that each of the factors that multiply the integrals in (27) are equal to one and the inequality becomes

$$K\int_{F_I}|\phi_3(x,0)|^2\,\mathrm{d}x \le \frac{(1+\epsilon)k^3|B_3|^2\sin 2k(b-a)}{K} + \int_{D_I}|\nabla\phi_3|^2\,\mathrm{d}V. \quad (29)$$

If the non-dimensional length of the free surface between the two structures lies in the range given by $(2n-1)\pi \le 2k(b-a) \le 2n\pi$, n integer, then $\sin 2k(b-a) \le 0$ and (29) becomes

$$K \int_{F_I} |\phi_3(x,0)|^2 \, \mathrm{d}x \le \int_{D_I} |\nabla \phi_3|^2 \, \mathrm{d}V. \tag{30}$$

This may be substituted into (17) to give

$$\mu_{33} \ge \frac{1}{A_0} \left[\int_{D_I} |\nabla \phi_3|^2 \, \mathrm{d}V - K \int_{F_I} |\phi_3|^2 \, \mathrm{d}x \right] \ge 0, \quad (2n-1)\pi \le 2k(b-a) \le 2n\pi, \tag{31}$$

where n is an integer.

For sway or roll motion ϕ_p is antisymmetric in x. So from (18) and (19)

$$w_p(x) = \int_{-\infty}^{0} \phi_p(x,z) \frac{\cosh k(z+h)}{\cosh kh} \, \mathrm{d}z = B_p \sin kx, \quad x \in F_I, \quad p = 1, 5. \tag{32}$$

A similar analysis to that used for symmetric motion produces a modified version of the inequality in (29), namely

$$K \int_{F_I} |\phi_p(x,0)|^2 \, \mathrm{d}x \le -\frac{(1+\epsilon)k^3 |B_p|^2 \sin 2k(b-a)}{K} + \int_{D_I} |\nabla \phi_p|^2 \, \mathrm{d}V, \quad p = 1, 5. \tag{33}$$

If $2n\pi \le 2k(b-a) \le (2n+1)\pi$, n integer, then $\sin 2k(b-a) \ge 0$ and (33) yields

$$K \int_{F_I} |\phi_p(x,0)|^2 \, \mathrm{d}x \le \int_{D_I} |\nabla \phi_p|^2 \, \mathrm{d}V, \quad p = 1, 5. \tag{34}$$

This may be substituted into (17) to give, for $p = 1$ or 5,

$$\mu_{pp} \ge \frac{1}{A_0} \left[\int_{D_I} |\nabla \phi_p|^2 \, \mathrm{d}V - K \int_{F_I} |\phi_p|^2 \, \mathrm{d}x \right] \ge 0, \quad 2n\pi \le 2k(b-a) \le (2n+1)\pi, \tag{35}$$

where n is an integer.

From (31) and (35), the ranges of frequency in which the added mass can possibly be negative, are complementary for symmetric and antisymmetric motion. It is worth noting that the theory only establishes that the added mass is non-negative in certain intervals, not that it takes negative values outside those intervals. In general the added mass is not negative everywhere outside these ranges. Numerical results obtained by a boundary element method (BEM) are presented in figure 4 for a pair of surface-piercing semi-circular cylinders in water of infinite depth. The

shaded areas represent the intervals in which the sway added mass has been proven to be non-negative and the heave added mass is non-negative in the complementary unshaded regions. It is clear that the numerical results are in agreement with the theoretical predictions, although the regions over which negative added mass occurs are observed to get closer and closer to the boundaries of the relevant intervals, as the frequency increases. In the next section, for fluid of infinite depth an approximate prediction is given of where the poles in the force coefficient occur, and hence the frequencies at which there are sign changes in the added mass.

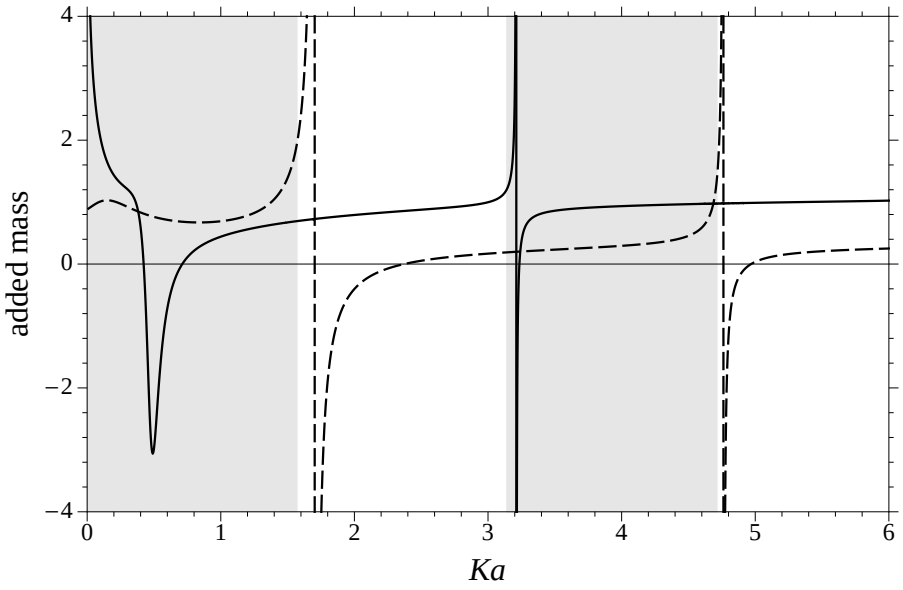

Figure 4: The heave —— and sway − − − added mass for 2 semi-circular cylinders, radius a, $b = 2a$

4. Approximations to the complex resonances

In this section the fluid is taken to have infinite depth so that both the wide-spacing theory described in [21], and certain high-frequency asymptotic results, may be used. The rapid changes in the added mass seen in figure 4 are associated with so-called complex resonances of the complex force coefficient

$$q_{pp}(\kappa) = \mu_{pp}(\kappa) + \mathrm{i}\nu_{pp}(\kappa) \tag{36}$$

where $\kappa = Ka$. With κ regarded as a complex variable, a complex resonance is a pole of $q_{pp}(\kappa)$, located in the lower half of the complex κ plane [14]. The pole is

assumed to be simple and, although the numerical evidence suggests that this is the case here, to the authors' knowledge it has not been established formally that it is necessarily true. Specifically, for a resonance at $\kappa = \kappa_n + \mathrm{i}\tau_n$ indexed by an integer n, with $\kappa_n, \tau_n \in \mathbb{R}$ and $\tau_n < 0$, then

$$q_{pp}(\kappa) \sim \frac{\widehat{q}_{pp,n}}{\kappa - (\kappa_n + \mathrm{i}\tau_n)} \quad \text{as} \quad \kappa \to \kappa_n + \mathrm{i}\tau_n, \tag{37}$$

where the residue $\widehat{q}_{pp,n}$ is a complex constant.

In the following it is assumed that the resonance under consideration is sufficiently close to the real axis for (37) to provide a good approximation to the complex force coefficient when κ is real and close to κ_n. Numerical calculations presented below indicate that $\mathrm{Re}\{\widehat{q}_{pp,n}\} < 0$ and $\mathrm{Im}\{\widehat{q}_{pp,n}\} \approx 0$, both of which are consistent with the requirement that the damping coefficient is non-negative. If (37) with $\widehat{q}_{pp,n} \in \mathbb{R}$ is adopted as an approximation near a resonance this gives

$$\mathrm{Re}\left\{q_{pp}(\kappa)\right\} = \mu_{pp}(\kappa) \approx \frac{\widehat{q}_{pp,n}(\kappa - \kappa_n)}{(\kappa - \kappa_n)^2 + \tau_n^2}. \tag{38}$$

This form describes the characteristic spikes in the added mass that are seen in figure 4. There are turning points in the added mass at $\kappa = \kappa_n \pm \tau_n$ at which $\mu_{pp} = \pm\widehat{q}_{pp,n}/2\tau_n$, hence the height of a spike is determined by the relevant residue and the distance of the pole from the real axis. Furthermore, on the basis of this approximation $\mu_{pp}(\kappa_n) = 0$, and these are the zeros observed on the downward parts of the curves in figure 4. The form (37) also yields a maximum value of the damping coefficient of $\widehat{q}_{pp,n}/\tau_n$ at $\kappa = \kappa_n$ so that the height of a spike in the damping is, to a first approximation, equal to the total height of the corresponding spike in the added mass [13].

4.1. Locations of the complex resonances

Approximations to the locations of the poles for a pair of surface-piercing structures may be obtained by adopting the assumption that the structures are widely spaced. Under the extended wide-spacing approximation [21, equations (6.16) and (6.18)], for two identical symmetric structures a distance $l = 2b$ apart resonances occur at those complex K for which

$$1 \mp r\,\mathrm{e}^{\mathrm{i}Kl} - \epsilon^2 p_3 \mathrm{e}^{\mathrm{i}Kl} = 0 \tag{39}$$

where, in the second term, the negative sign is taken for symmetric motions and the positive sign for antisymmetric motions, r is the reflection coefficient for a single

isolated structure and $\epsilon = 1/Kl$. It is assumed that $r \neq 0$ for the frequencies under consideration. In the extended wide-spacing approximation it is assumed that $\epsilon \ll 1$ and $a/b \ll 1$, where a is a typical dimension of each structure. Further p_3, defined in [21, equations (5.8)], is a property of a single isolated structure that depends on frequency. Thus, both r and p_3 are functions of the real frequency parameter $\kappa = Ka$ and, for the present purposes, each may be extended analytically into a suitable complex neighbourhood of the real axis (see [14, section 4]). Results will be obtained using the standard wide-spacing approximation ($\epsilon = 0$); the term in ϵ^2 is included above to shed light on the magnitude of the first neglected term and will not be be included explicitly from now on (for the case of a half-immersed circular cylinder next to a wall, the effects of this term are discussed in detail in [22]). The overall aim is to obtain approximations to the locations of resonances using high-frequency approximations to the hydrodynamic coefficients that are valid for $Ka \gg 1$. The wide-spacing approximation is effectively an expansion in the small parameter $1/Kb$, and hence it is consistent to expand individual terms in $1/Ka$ as long as $1/Kb \ll 1/Ka$, which is just a rewriting of the second wide-spacing assumption $a/b \ll 1$.

From equation (39), as $\epsilon \to 0$

$$\mathrm{e}^{-2\mathrm{i}\kappa\, b/a + n\pi\mathrm{i}} = r + O(\epsilon^2), \tag{40}$$

where the integer n is even for symmetric motions and odd for antisymmetric motions, and hence

$$-2\mathrm{i}\kappa\, b/a + n\pi\mathrm{i} = \log r + O(\epsilon^2). \tag{41}$$

For surface-piercing structures, it is anticipated that the complex resonances are close to the real axis and hence, for a chosen n, equation (41) has a solution $\kappa = \kappa_n + \mathrm{i}\tau_n$, where $\kappa_n, \tau_n \in \mathbb{R}$ and $|\tau_n| \ll |\kappa_n|$. By Taylor expansion

$$r(\kappa) = r(\kappa_n) + \mathrm{i}\tau_n r'(\kappa_n) + O(\tau_n^2) \quad \text{as} \quad \tau_n \to 0 \tag{42}$$

where, by a result from complex analysis, it is permissible to take the derivative r' in the real κ direction. Thus equation (41) becomes

$$-2\mathrm{i}(\kappa_n + \mathrm{i}\tau_n)b/a + n\pi\mathrm{i} = \log r + \frac{\mathrm{i}\tau_n r'}{r} + O(\tau_n^2, \epsilon^2), \tag{43}$$

where r and r' are now evaluated at $\kappa = \kappa_n$. The real part of equation (43) yields

$$\tau_n \left(\frac{2b}{a} + \operatorname{Im} \frac{r'}{r} \right) = \log |r| + O(\tau_n^2, \epsilon^2), \tag{44}$$

while the imaginary part gives

$$2\kappa_n b/a = n\pi - \delta_r - \tau_n \operatorname{Re}\frac{r'}{r} + O(\tau_n^2, \epsilon^2), \tag{45}$$

where $\delta_r = \arg r$.

Approximations to r are available for a number of geometries. For example, Leppington [23] considers the reflection of waves by cylinders whose cross section B' intersects the free surface normally; he further assumes that B' is locally smooth and convex at the two intersection points (see [23, p. 134] for an explanation of the reasons for this). Suppose that near the intersection points $x = \pm a$, B' has the local form

$$x \mp a = \mp \sum_{s=N}^{\infty} \frac{\alpha_s (-z)^s}{s!}, \tag{46}$$

where $2 \leq N < \infty$ and to ensure local convexity $\alpha_N > 0$. From [23] the reflection coefficient

$$r \sim \left(1 - \frac{\mathrm{i}\alpha_N a^{N-1}}{(2\kappa)^{N-1}}\right) \mathrm{e}^{-2\mathrm{i}\kappa} \quad \text{as} \quad \kappa \to \infty \tag{47}$$

and the transmission coefficient

$$t \sim \frac{t_0 \mathrm{e}^{-2\mathrm{i}\kappa}}{\kappa^{2N}} \quad \text{as} \quad \kappa \to \infty, \tag{48}$$

where the constant t_0 is determined by the geometry of B'; it follows from (47) that the phase

$$\delta_r \sim -2\kappa - \frac{\alpha_N a^{N-1}}{(2\kappa)^{N-1}} \quad \text{as} \quad \kappa \to \infty. \tag{49}$$

The leading-order approximation to $\log|r|$ is obtained from t using the identity $|r|^2 + |t|^2 = 1$ so that from (44)

$$\tau_n(b/a - 1) \approx -\frac{|t_0|^2}{4\kappa_n^{4N}}. \tag{50}$$

It then follows from (45) that

$$\kappa_n(b/a - 1) \approx \tfrac{1}{2} n\pi + \frac{\alpha_N a^{N-1}}{2^N \kappa_n^{N-1}} \tag{51}$$

or, after reversion,

$$\kappa_n(b/a-1) \approx \tfrac{1}{2}n\pi + \tfrac{1}{2}\alpha_N \left[\frac{b-a}{n\pi}\right]^{N-1}. \tag{52}$$

Other than the dependence on n, these approximations do not depend on the flow symmetry of the resonance under consideration.

The first approximation $\kappa_n(b/a-1) \approx \frac{1}{2}n\pi$ corresponds to the the right-hand end of a region for which, in section 3.2, it has been shown that negative added mass does *not* occur. The second term in (52) then shifts the real part of the complex resonance to a higher frequency which is consistent with the theory of section 3.2 (recall the remark above that the zeros on the downward parts of the added-mass curves occur, to a first approximation, at $\kappa = \kappa_n$). As a specific example suppose that B' is a semicircle of radius a. From results given in [23, section 4], for this case $N = 2$, $\alpha_2 = 1/a$ and $t_0 = 2\mathrm{i}/\pi$ so that

$$\kappa_n(b/a-1) \approx \tfrac{1}{2}n\pi + \frac{b/a-1}{2n\pi} \tag{53}$$

and

$$\tau_n(b/a-1) \approx -\frac{1}{\pi^2\kappa_n^8}. \tag{54}$$

The accuracy of these approximations is assessed by comparison with numerical results in section 4.3 below.

Suitable high-frequency results for other classes of geometry are also available. For example, Ayad & Leppington [24] consider high-frequency scattering by cylinders that intersect the free surface in vertical planes. In this case, both $\delta_r + 2\kappa$ and t are exponentially small as $\kappa \to \infty$, and hence τ_n and $\kappa_n(b/a-1) - \frac{1}{2}n\pi$ are also exponentially small (the latter quantity is again positive to a first approximation).

4.2. Residues

The residues at simple poles of $q(\kappa)$ in the complex plane may be estimated as follows. Suppose that

$$q_{pp}(\kappa) = \frac{f_{pp}(\kappa)}{g_{pp}(\kappa)} \tag{55}$$

where $g_{pp}(\kappa)$ has a simple zero at $\kappa = \widehat{\kappa}$ and $f_{pp}(\widehat{\kappa}) \neq 0$, so that $q_{pp}(\kappa)$ has a simple pole at $\kappa = \widehat{\kappa}$. The residue at the pole is

$$\widehat{q}_{pp} = \lim_{\kappa\to\widehat{\kappa}} \frac{(\kappa-\widehat{\kappa})f_{pp}(\kappa)}{g_{pp}(\kappa)} = \frac{f_{pp}(\widehat{\kappa})}{g'_{pp}(\widehat{\kappa})}, \tag{56}$$

where prime denotes differentiation. For a resonance, that is a simple pole of q_{pp}, at $\widehat{\kappa} = \kappa_n + \mathrm{i}\tau_n$ the residue

$$\widehat{q}_{pp,n} = \frac{f_{pp}(\kappa_n)}{g'_{pp}(\kappa_n)} + O(\tau_n) \quad \text{as} \quad \tau_n \to 0. \tag{57}$$

Denote by $q_{1,pp}$ the complex force coefficient for a single structure in isolation, and by A_p the amplitude of waves radiated by a single structure and scaled by a. From [21, equations (3.8), (6.16) and (6.18)], for sway

$$q_{11}(\kappa) = 2q_{1,11}(\kappa) + \frac{2\mathrm{i}\mathrm{e}^{2\mathrm{i}\kappa b/a}[A_1(\kappa)]^2}{\pi[1 + r(\kappa)\,\mathrm{e}^{2\mathrm{i}\kappa b/a}]} \tag{58}$$

and for heave

$$q_{33}(\kappa) = 2q_{1,33}(\kappa) - \frac{\mathrm{i}\mathrm{e}^{2\mathrm{i}\kappa b/a}[A_3(\kappa)]^2}{\pi[1 - r(\kappa)\,\mathrm{e}^{2\mathrm{i}\kappa b/a}]} \tag{59}$$

(factors of π have been introduced into the denominators because a different non-dimensionalisation was used in [21]). From the high-frequency asymptotics of the reflection coefficient given in equation (47), the leading approximations to the residues are therefore

$$\widehat{q}_{11,n}(\kappa) \approx \frac{\mathrm{e}^{2\mathrm{i}\kappa_n}[A_1(\kappa_n)]^2}{\pi(b/a - 1)} \quad \text{and} \quad \widehat{q}_{33,n}(\kappa) \approx \frac{\mathrm{e}^{2\mathrm{i}\kappa_n}[A_3(\kappa_n)]^2}{2\pi(b/a - 1)}. \tag{60}$$

For the semicircle, Simon [25] gives that as $\kappa \to \infty$

$$A_1 \sim -\frac{2\mathrm{i}\mathrm{e}^{-\mathrm{i}\kappa}}{\kappa} \quad \text{and} \quad A_3 \sim -\frac{4\mathrm{i}\mathrm{e}^{-\mathrm{i}\kappa}}{\kappa^2} \tag{61}$$

so that, in this case,

$$\widehat{q}_{11,n}(\kappa) \approx -\frac{4}{\pi(b/a - 1)\kappa_n^2} \quad \text{and} \quad \widehat{q}_{33,n}(\kappa) \approx -\frac{8}{\pi(b/a - 1)\kappa_n^4}. \tag{62}$$

Both approximate residues are real, which is consistent with the requirement that the damping is non-negative.

As noted above, first approximations to the extreme values of the added mass are $\pm\widehat{q}_{pp,n}/2\tau_n$. Thus, for sway the extreme values are $\pm 2\pi\kappa_n^6$ and for heave they are $\pm 4\pi\kappa_n^4$ so that the height of the sway spikes grows more rapidly with increasing frequency. This behaviour explains why in figure 4 the second sway spike appears

n	1	2	3
$\frac{1}{2}n\pi$	1.571	3.142	4.712
κ_n (BEM)	1.703	3.218	4.762
κ_n (approx)	1.730	3.221	4.765
τ_n (BEM)	$-(3.3 \pm 0.3) \times 10^{-4}$	$-(1.1 \pm 0.1) \times 10^{-5}$	$-(2.8 \pm 1.3) \times 10^{-7}$
τ_n (approx)	-1.3×10^{-3}	-8.7×10^{-6}	-3.8×10^{-7}
$\widehat{q}_{pp,n}$ (BEM)	-0.21 ± 0.01	-0.021 ± 0.005	-0.055 ± 0.001
$\widehat{q}_{pp,n}$ (approx)	-0.425	-0.024	-0.056

Table 1: Resonances: comparison of boundary element method (BEM) calculations with the approximate formulae (53), (54) and (62) for two half-immersed cylinders with $b/a = 2$.

somewhat broader than the second heave spike; it is simply a much larger spike. In fact, for the heave spike the maximum added mass is about 1350 while for the sway spike it is about 74,000. This behaviour may interpreted in terms of the wave making properties of a single half-immersed cylinder; at high frequencies a swaying cylinder generates waves more readily than a heaving cylinder (see equation (61)), and hence interactions between two cylinders are stronger for synchronised sway when compared with synchronised heave.

4.3. Comparison with the BEM calculations

The above approximations are now compared with the BEM calculations presented previously. The resonances and their corresponding residues were computed from the BEM results using an adaptation of the technique described in [26]. In that paper, a Taylor series expansion of the complex force coefficient about the frequency corresponding to a maximum in the damping coefficient was used. However, the extreme height and narrowness of the resonance spikes for the geometry used here mean that this choice of expansion point is not practical. Instead, a range of expansion frequencies covering the shoulders of the resonance spikes was used to obtain the results given in table 1. This gives a range of values for each quantity and hence allows an error estimate to be obtained. The results in figure 4 indicate that there are four resonances within the range of κ displayed – two associated with heave and two with sway – and these are assigned the indices $n = 0..3$ in increasing order of frequency. (The roll resonances occur at the same frequencies as the sway resonances although the residues are different.) The first heave resonance $n = 0$ is

at a sufficiently low frequency for the behaviour of the added mass to be strongly influenced by the singular behaviour of the added mass at zero frequency. As a consequence, reliable numerical estimates for $n = 0$ cannot be obtained and hence do not appear in table 1 (furthermore, the wide-spacing theory of section 4.1 does not apply in this case). Results for the remaining heave resonance ($n = 2$) and the two sway resonances ($n = 1, 3$) do appear in the table. For the real parts κ_n of the resonance frequencies reliable numerical results to three decimal places are obtained; in each case these values of κ_n correspond, to the number of digits shown, with the locations of the zeros on the downward portions of the added mass curves computed by the BEM. The imaginary parts τ_n are small and the most difficult to estimate numerically (indeed, for $n = 3$ the first digit was not obtained reliably). Only the real parts of the residues are given; the BEM computations do suggest that there is a small non-zero imaginary part. These results indicate that, at least for the geometry under consideration, the combination of the wide-spacing approximation with high-frequency asymptotics is able to give useful approximations to the resonances.

4.4. Approximations away from the resonances

Adopting the above high-frequency approximations for the half-immersed circle directly in equations (58) and (59), but with the assumption that κ is not close to a resonance so that there is no zero in the denominator, yields the approximations to the interaction terms:

$$q_{11}(\kappa) - 2q_{1,11}(\kappa) \approx -\frac{4}{\pi\kappa^2}\left(-\tan[\kappa(b/a-1)] + \mathrm{i}\right) \tag{63}$$

and

$$q_{33}(\kappa) - 2q_{1,33}(\kappa) \approx -\frac{8}{\pi\kappa^4}\left(\cot[\kappa(b/a-1)] + \mathrm{i}\right). \tag{64}$$

Within the high-frequency regime, these expressions broadly describe the behaviour seen in figure 4. In both cases, at high frequencies the interactions act to decrease the damping of a cylinder pair compared to twice the values for a single cylinder. This is because some of the energy radiated by the cylinders individually is trapped between the cylinders, and hence cannot reach infinity.

5. Discussion

In this paper, it has been shown that the diagonal coefficients in the added mass matrix, are not negative at any frequency, for a single two-dimensional structure that satisfies the so-called John condition. Unfortunately it is not possible to extend this

argument, to single structures that are contained within lines that do not intersect the free surface perpendicularly, in the way that John's uniqueness argument was extended in [27] and [20, §3.2.2]. Mathematically this is because in the analysis of the uniqueness problem, similar inequalities to those given in (13) and (14) arise, with ϕ_p replaced by the real solution of the homogeneous boundary value problem, but with an extra factor on the right-hand side of each inequality, that is less than one. This provides scope for changing the orientation or shape of the lines that connect the free surface to the seabed in $D_{\pm}$, in such a way that when the extension of John's argument is made, this factor increases to a maximum of one. As the factor already takes the maximum possible value in this work, there is not the same possibility for extension of the argument. In fact there is not a one-to-one correspondence between uniqueness of potential and non-negative added mass, as illustrated in Figure 2, where the sway added mass for a circular cylinder that is more than half-immersed in water of infinite depth and intersects the mean free surface at an angle of $\pi/4$ to the horizontal, is seen to take negative values in a certain frequency range. This is a structure for which the extended version of John's argument [27] establishes uniqueness of potential at all frequencies.

In general, the added mass is negative at some frequencies for a horizontally separated pair of structures. However, for a symmetric arrangement of bodies that individually satisfy the John condition, it was shown in the present work that the added mass is non-negative in certain complementary ranges of frequency, for symmetric and antisymmetric motions. In addition, a wide-spacing approximation was used to confirm the close connection between complex resonances and negative added mass in two-dimensional problems. An extension to slender toroidal geometries may be possible by coupling the wide-spacing approximation with strip theory (see [10]) so that the extensive high-frequency results for two-dimensional geometries could again be used.

Further extensions to three dimensions will be considered in a separate paper where single axisymmetric bodies without an internal free surface that also satisfy the John condition will be studied, as will toroidal 'John' bodies that enclose a portion of the free surface. By analogy with the three-dimensional uniqueness results described in [20, §4.2.3], it is expected that in the former case the diagonal added mass coefficients must be non-negative for all frequencies, while in the latter case non-negative values can be expected only in particular ranges of frequency.

6. References

[1] C. M. Linton, P. McIver, Handbook of Mathematical Techniques for Wave/Structure Interactions, Chapman & Hall/CRC, Boca Raton, 2001.

[2] T. F. Ogilvie, First- and second-order forces on a cylinder submerged under a free surface, J. Fluid Mech. 16 (1963) 451–472.

[3] J. N. Newman, B. Sortland, T. Vinje, Added mass and damping of rectangular bodies close to the free surface, J. Ship Res. 28 (4) (1984) 219–225.

[4] P. McIver, D. V. Evans, The occurrence of negative added mass in free-surface problems involving submerged oscillating bodies, J. Engng Maths 18 (1984) 7–22.

[5] P. A. Martin, L. Farina, Radiation of water waves by a heaving submerged horizontal disc, J. Fluid Mech. 337 (1997) 365–379.

[6] S. Wang, R. Wahab, Heaving oscillations of twin cylinders in a free surface, J. Ship Res. 15 (1971) 33–48.

[7] O. M. Faltinsen, O. F. Rognebakke, A. N. Timokha, Two-dimensional resonant piston-like sloshing in a moonpool, J. Fluid Mech. 575 (2007) 359–397.

[8] R. W. Yeung, R. K. M. Seah, On Helmholtz and higher-order resonance of twin floating bodies, J. Engng Maths 58 (2007) 251–265.

[9] R. Porter, D. Evans, Estimation of wall effects on floating cylinders, J. Engng Maths 70 (2011) 191–204.

[10] J. N. Newman, The motions of a floating slender torus, J. Fluid Mech. 83 (1977) 721–735.

[11] J. N. Newman, Radiation and diffraction analysis of the McIver toroid, J. Engng Maths 35 (1999) 135–147.

[12] S. A. Mavrakos, Hydrodynamic coefficients in heave of two concentric surface-piercing truncated circular cylinders, Appl. Ocean Res. 26 (2004) 84–97.

[13] C. M. Linton, D. V. Evans, Hydrodynamic characteristics of bodies in channels, J. Fluid Mech. 252 (1993) 647–666.

[14] P. McIver, Complex resonances in the water-wave problem for a floating structure, J. Fluid Mech. 536 (2005) 423–443.

[15] M. McIver, The scattering properties of a system of structures in water waves, Q. J. Mech. Appl. Maths 67 (4) (2014) 631–639.

[16] F. John, On the motion of floating bodies, II. Simple harmonic motions, Communications Pure Applied Mathematics 3 (1950) 45–101.

[17] J. Falnes, P. McIver, Surface wave interactions with systems of oscillating bodies and pressure distributions, Appl. Ocean Res. 7 (1985) 225–234.

[18] C. M. Linton, N. G. Kuznetsov, Non-uniqueness in two-dimensional water-wave problems: numerical evidence and geometrical restrictions, Proc. Roy. Soc. Lond. A 453 (1997) 2437–2460.

[19] M. McIver, P. McIver, The sign of the added mass coefficients for 2-d structures, in: Proc. 30th Intl. Workshop on Water Waves and Floating Bodies, Bristol, UK, 2015, pp. 145–148.

[20] N. Kuznetsov, V. Maz'ya, B. Vainberg, Linear Water Waves, Cambridge University Press, 2002.

[21] P. McIver, An extended wide-spacing approximation for two-dimensional water-wave problems in infinite depth, Q. J. Mech. Appl. Maths 67 (3) (2014) 445–468.

[22] P. McIver, R. Porter, The motion of a freely-floating cylinder next to a wall and the approximation of resonances, Submitted.

[23] F. G. Leppington, On the radiation and scattering of short surface waves. Part 2, J. Fluid Mech. 59 (1973) 129–146.

[24] A. M. Ayad, F. G. Leppington, The diffraction of surface waves by plane vertical obstacles, J. Fluid Mech. 80 (3) (1977) 593–604.

[25] M. Simon, The high-frequency radiation of water waves by oscillating bodies, Proc. Roy. Soc. Lond. A 401 (1985) 89–115.

[26] C. J. Fitzgerald, P. McIver, Approximation of near-resonant wave motion using a damped harmonic oscillator model, Appl. Ocean Res. 31 (2009) 171–178.

[27] M. J. Simon, F. Ursell, Uniqueness in linearized two-dimensional water-wave problems, J. Fluid Mech. 148 (1984) 137–154.